



Differential associations of metabolic risk factors on cortical thickness in metabolic syndrome



Nicolette F. Schwarz^{a,b}, Leslie K. Nordstrom^{a,b}, Linda H.G. Pagen^{a,b,1}, Daniela J. Palombo^{a,c}, David H. Salat^{a,b,d}, William P. Milberg^{a,b}, Regina E. McGlinchey^{a,b}, Elizabeth C. Leritz^{a,b,*}

^a Neuroimaging Research for Veterans Center (NeRVe), Geriatric Research Education and Clinical Center (GRECC), Veterans Administration Boston Healthcare System, Boston, MA, USA

^b Harvard Medical School, Boston, MA, USA

^c Boston University School of Medicine, Boston, MA, USA

^d The Athinoula A. Martinos Center for Biomedical Imaging, Boston, MA, USA

ARTICLE INFO

Keywords:

Obesity
Dyslipidemia
Hyperglycemia
Diastolic blood pressure
Gray matter
Magnetic resonance imaging

ABSTRACT

Objective: Metabolic syndrome (MetS) refers to a cluster of risk factors for cardiovascular disease, including obesity, hypertension, dyslipidemia, and hyperglycemia. While sizable prior literature has examined associations between individual risk factors and quantitative measures of cortical thickness (CT), only very limited research has investigated such measures in MetS. Furthermore, the relative contributions of these risk factors to MetS-related effects on brain morphology have not yet been studied. The primary goal of this investigation was to examine how MetS may affect CT. A secondary goal was to explore the relative contributions of individual risk factors to regional alterations in CT, with the potential to identify risk factor combinations that may underlie structural changes.

Methods: Eighteen participants with MetS (mean age = 59.78 years) were age-matched with 18 healthy control participants (mean age = 60.50 years). CT measures were generated from T1-weighted images and groups were contrasted using whole-brain general linear modeling. A follow-up multivariate partial least squares correlation (PLS) analysis, including the full study sample with complete risk factor measurements (N = 53), was employed to examine which risk factors account for variance in group structural differences.

Results: Participants with MetS demonstrated significantly reduced CT in left hemisphere inferior parietal, rostral middle frontal, and lateral occipital clusters and in a right hemisphere precentral cluster. The PLS analysis revealed that waist circumference, high-density lipoprotein cholesterol (HDL-C), triglycerides, and glucose were significant contributors to reduced CT in these clusters. In contrast, diastolic blood pressure showed a significantly positive association with CT while systolic blood pressure did not emerge as a significant contributor. Age was not associated with CT.

Conclusion: These results indicate that MetS can be associated with regionally specific reductions in CT. Importantly, a novel link between a risk factor profile comprising indices of obesity, hyperglycemia, dyslipidemia and diastolic BP and localized alterations in CT emerged. While the pathophysiological mechanisms underlying these associations remain incompletely understood, these findings may be relevant for future investigations of MetS and might have implications for treatment approaches that focus on specific risk factor profiles with the aim to reduce negative consequences on the structural integrity of the brain.

1. Introduction

Metabolic syndrome (MetS) is defined as the constellation of three or more risk factors for atherosclerotic cardiovascular disease and type

2 diabetes mellitus (Eckel et al., 2005; Grundy, 2007). Component risk factors may include abdominal obesity, hypertension, dyslipidemia (low levels of high-density lipoprotein cholesterol (HDL-C) and high levels of triglycerides), and hyperglycemia (high levels of glucose)

Abbreviations: MetS, Metabolic Syndrome; HDL-C, high-density lipoprotein cholesterol; CT, cortical thickness; BP, blood pressure; PLS, partial least squares correlation; MRI, magnetic resonance imaging; VA, Veterans Administration Boston Healthcare System; GLM, general linear model; FDR, false discovery rate

* Corresponding author at: VA Boston Healthcare System, 150 S Huntington Ave, Boston, MA 02130, USA.

E-mail address: Elizabeth.Leritz@hms.harvard.edu (E.C. Leritz).

¹ Maastricht University, Faculty of Health, Medicine, and Life Sciences, Maastricht, Netherlands.

<http://dx.doi.org/10.1016/j.nicl.2017.09.022>

Received 5 April 2017; Received in revised form 31 August 2017; Accepted 26 September 2017

Available online 28 September 2017

2213-1582/ © 2017 Published by Elsevier Inc. This is an open access article under the CC BY-NC-ND license (<http://creativecommons.org/licenses/by-nc-nd/4.0/>).

(Grundy, 2005). There is considerable evidence that the presence of MetS imparts augmented risk for stroke, cerebrovascular disease, cognitive decline, and dementia (Maruyama et al., 2009; Park and Kwon, 2008; Raffaitin et al., 2009; Wild et al., 2009; Yaffe, 2007; Yates et al., 2012). However, while the individual risk factors that comprise MetS have been linked to alterations in the structural integrity of the brain, less is known about the effects of MetS per se on brain structure (Friedman et al., 2014). Highly prevalent in the adult U.S. American population, with estimates ranging between 23% and 35%, MetS is projected to remain a serious public health concern (Aguilar et al., 2015; Beltrán-Sánchez et al., 2013; Grundy, 2008). Therefore, it is critical to understand how MetS affects brain structural integrity, particularly since its component risk factors can be modified via lifestyle changes and pharmaceutical treatment (Eckel et al., 2005; Grundy, 2007).

The component risk factors have been linked to brain tissue alterations in both white and gray matter (Friedman et al., 2014; Leritz et al., 2011; Salat et al., 2012; Tchistiakova et al., 2016; Veit et al., 2014; Vuorinen et al., 2013; Williams et al., 2013). As a sensitive marker of gray matter integrity, cortical thickness (CT) can provide information on cortical atrophy and has been employed in studies of cognitive function (Preul et al., 2005; Tchistiakova et al., 2016), aging (Fjell et al., 2009; Salat et al., 2004), neurodegenerative disease (Jacobs et al., 2014; Seo et al., 2012), small vessel disease (Preul et al., 2005; Reid et al., 2010), type 2 diabetes mellitus (Brundel et al., 2010; Tchistiakova et al., 2014), as well as in individual MetS risk factors (Alisco et al., 2014; Brundel et al., 2010; Hassenstab et al., 2012; Krishnadas et al., 2013; Leritz et al., 2011; Seo et al., 2012; van Velsen et al., 2013; Veit et al., 2014; Vuorinen et al., 2013). Using this metric to investigate neural health in generally healthy older adults, Leritz et al. (2011) reported significant negative associations between intra-individual variations in blood pressure (BP) factor scores (comprising systolic and diastolic BP) and quantitative measures of CT in frontal and temporal regions. In contrast, they also observed significant positive associations between a cholesterol factor (comprising total cholesterol and low-density lipoprotein cholesterol) and CT in widespread regions that prominently included frontal, parietal, and temporal cortices. Positive relationships in similar regions were reported for other lipid factors (Krishnadas et al., 2013), for visceral fat in adolescents (Saute et al., 2016), and for central adiposity in right posterior cingulate gyrus (Kaur et al., 2015a). Only a very limited number of studies have been published that have examined CT specifically in MetS cohorts, reporting regionally reduced CT in left insular, postcentral, and entorhinal and in bilateral superior parietal regions (Song et al., 2015). More recently, McIntosh et al. (2017) reported reduced CT of both hemispheres as well as in bilateral medial temporal lobe structures, which were chosen as regions of interest, relative to control groups. Similar observations have been made in related cohorts, for example, higher empirically-derived MetS severity scores (representing individual differences in MetS severity) were associated with reduced CT in orbitofrontal, temporal, cingulate, and occipital regions in U.S. military veterans (Wolf et al., 2016). Another study found that a greater number of MetS risk factors was associated with reduced CT in an inferior frontal region (Kaur et al., 2015b), although that relationship was mediated by a marker of inflammation. Furthermore, a greater number of vascular risk factors (represented as summative indices) was related to reduced CT measures in frontal and temporal regions in participants with mild cognitive impairment (Tchistiakova et al., 2016). Taken together, studies with both individual risk factors and with MetS suggest that vascular risk may affect CT in a regionally specific manner, including frontal, temporal and parietal regions. Given the sparse literature, it is currently not well understood in which way the component and co-occurring risk factors might contribute to these changes.

Composite measures like severity scores and risk factor counts, however, make it more difficult to assess which MetS components might be contributing more to altered gray matter integrity than others.

Indeed, this is an important direction as empirical factor analytic studies have shown that MetS risk factors tend to cluster in specific patterns (Meigs, 2000; Wolf et al., 2016). For example, indices of insulin resistance (e.g., fasting blood insulin and glucose) often load on those factors that include measures of hyperglycemia, obesity, or dyslipidemia, and importantly, they load on more than one factor across studies (Gray et al., 1998; Hanley et al., 2002; Hanson et al., 2002; Meigs, 2000; Meigs et al., 1997; Sakkinen et al., 2000; Shen et al., 2003). Interestingly, BP most often emerges as a unique factor that only infrequently loads together with other variables (Hanley et al., 2002; Meigs, 2000; Sakkinen et al., 2000). That these studies yield more than one factor on which these variables converge suggests that there are separate disease mechanisms involved (Meigs, 2000). Examining whether there are particular patterns in which risk factors are related to alterations in CT might provide novel information on underlying pathophysiological processes in MetS. Accordingly, here we extend prior investigations and explore the relative contributions of component risk factors, in context of each other, to identify associations to CT in a MetS cohort.

The current cross-sectional study aimed to examine the integrity of cerebral gray matter, measured as CT across the entire cortical mantle, in participants with MetS. Based on prior findings in MetS and related cohorts and considerable literature examining the individual risk factors, we hypothesized that, overall, individuals with MetS would demonstrate primarily reduced CT in frontal, temporal, and parietal cortices relative to a control group (Kaur et al., 2015b; Leritz et al., 2011; McIntosh et al., 2017; Song et al., 2015; Wolf et al., 2016). However, since positive associations between CT and lipid factors and adiposity have been reported as well, regionally greater CT might also be identified (Kaur et al., 2015a; Krishnadas et al., 2013; Leritz et al., 2011; Saute et al., 2016). Consequently, a second aim was to use a partial least squares correlation (PLS) analysis to determine *which* risk factors may be most affiliated with patterns of CT in MetS-related brain regions. In doing so, we hope to shed light on whether there are particular combinations of risk factors underlying a MetS diagnosis that are particularly detrimental to cortical gray matter integrity.

2. Methods

2.1. Participants

Thirty-six participants of an initial sample of 59 were included in the group comparison to determine regions of MetS-related CT alterations and 53 participants were included in subsequent PLS analyses. Individuals were enrolled from direct clinic recruitment via the Veterans Administration Healthcare Services to target those at high risk for MetS, as well as through advertisement in the greater Boston, Massachusetts (USA) metropolitan area. Inclusion criteria required participants to be English speakers and between the ages of 30–90. Exclusion criteria encompassed significant medical disease (e.g., overt cardiovascular disease), neurological disorders (e.g., Parkinson's disease or dementia), prior major surgery (e.g., brain or cardiac surgery), head trauma (e.g., loss of consciousness for > 30 min), history of severe or current psychiatric disorders (e.g., schizophrenia or major depressive disorder), history or current diagnosis of drug abuse or dependence, or any contraindication to magnetic resonance imaging (MRI).

From the initial sample of 59, four participants were excluded due to having insufficient physiological data to determine group assignment. The remaining cohort of 55 individuals was dichotomized into participants with and without MetS. While the HDL-C and waist circumference measurements were missing from two participants respectively, this did not affect group assignment as whether or not meeting MetS criteria could be determined from the remaining risk factor measures. Finally, 53 participants had a complete risk factor data set. MetS was defined as meeting thresholds for three or more of the following risk factors: 1) elevated waist circumference $\geq 102/88$ cm or

≥ 40/35 in (men/women), 2) elevated triglycerides ≥ 150 mg/dL or drug treatment for elevated triglycerides, 3) reduced HDL-C < 40/50 mg/dL (men/women) or drug treatment for reduced HDL-C, 4) elevated systolic BP ≥ 130 mm Hg or diastolic BP ≥ 85 mm Hg or drug treatment for hypertension, and 5) elevated fasting plasma glucose ≥ 100 mg/dL or drug treatment for elevated glucose (Grundy, 2005). Eighteen participants (33%) were identified as having MetS. Subsequently, 18 of the remaining 37 control participants (defined as having two or less risk factors) were pair-wise matched on age to the MetS participants to form a cohort of a total of 36 participants for the between-group comparison.

The study was approved and monitored by the Institutional Review Board of the Veterans Administration Boston Healthcare System (VA), Jamaica Plain, MA, USA. All participants provided informed consent prior to study procedures.

2.2. Assessment of participant characteristics

Waist circumference measurements were taken to the nearest centimeter after normal expiration with a measuring tape placed around the abdomen at the level of the umbilicus with the participant standing. Two systolic and diastolic BP measurements were acquired in the seated position after 5 min of rest, with the arm resting at the level of the heart, using a standard sphygmomanometer. The average of the two systolic BP values and the average of the two diastolic BP values were used in the analyses below. Triglycerides, HDL-C, and plasma glucose measurements were extracted from a fasting (12 h overnight) blood sample (Quest Diagnostics, Cambridge, MA, USA). Medications to treat hypertension, hyperglycemia, and dyslipidemia were recorded via self-report. A body mass index was calculated as kg/m² and presented only to enable comparison with previous literature (this measure was missing for one participant in the control group).

2.3. Structural data acquisition and analysis

2.3.1. Image acquisition

Two high-resolution 3D T1-weighted structural scans in the sagittal plane were acquired on 3 Tesla Siemens TIM TRIO scanners (Erlangen, Germany), employing a transmission body coil and a 32-channel reception head coil, using a magnetization prepared rapid acquisition gradient echo protocol (MPRAGE; repetition time = 2530 msec, echo time = 1.64 msec, inversion time = 1200 msec, flip angle = 7°, field of view = 256 × 256 mm, acquisition matrix 256 × 256, 176 contiguous slices, voxel size = 1 × 1 × 1 mm). Using the same scanner model and sequence parameters, 15/18 participants in the MetS group and 15/18 participants in the control group were scanned at the Athinoula A. Martinos Center for Biomedical Imaging, Charlestown, MA, USA. Study funding was shifted at this point, and therefore, the remaining participants were scanned at the VA. Sequences were copied and transferred from the Massachusetts General Hospital to the VA to minimize any scanner-related differences (Han et al., 2006; Wonderlick et al., 2009).

2.3.2. Cortical thickness estimation

CT measurements across the entire cerebral surface were obtained in a standardized and automated way using the “recon-all” pipeline of the open source FreeSurfer software suite (version 5.3.0, <http://surfer.nmr.mgh.harvard.edu>, Athinoula A. Martinos Center for Biomedical Imaging, Charlestown, MA, USA) (Fischl, 2012). Both structural scans were motion-corrected and averaged, yielding a single image volume with high contrast-to-noise ratio. This volume was then subjected to automated Talairach transformation, removal of non-brain tissue (Ségonne et al., 2004), segmentation of subcortical white matter and deep gray matter volumetric structures (Fischl et al., 2002; Fischl et al., 2004a), intensity normalization (Sled et al., 1998), and white matter segmentation. Surface processing included triangular tessellation of the

gray and white matter boundary, automated topology correction (Fischl et al., 2001; Ségonne et al., 2007), and surface deformation optimally placing the gray/white matter and gray matter/cerebral spinal fluid borders along shifts in intensity gradients across tissue classes (Dale et al., 1999; Dale and Sereno, 1993; Fischl and Dale, 2000). Resulting surface models were inspected for each participant and manually edited by a trained rater (LKN) when necessary (e.g., misclassification of gray/white matter boundaries). In case of edits, these models were re-estimated. Surfaces were then inflated, registered to a spherical atlas to enable comparison across participants (Fischl et al., 1999a; Fischl et al., 1999b) and cortical parcellations were derived (Destrieux et al., 2010; Fischl et al., 2004b).

A continuous measure of CT was calculated as the closest distance between the gray/white matter boundary to the gray matter/cerebrospinal fluid boundary at each vertex across the entire cortical mantle (Fischl and Dale, 2000). Only the thickness of the neocortical mantle (i.e., excluding subcortical structures such as thalamus) was included in the analysis. CT measurements were mapped and visualized on the pial surface of the participant's reconstructed brain and then smoothed across the surface using a circularly symmetric Gaussian kernel with a full width at half maximum of 10 mm (Dale and Sereno, 1993; Fischl et al., 1999a). Maps of individual participants were then averaged to provide an average measure of CT at each vertex. Since the gray matter boundary is estimated from the white matter boundary deforming outwards to the pial surface, FreeSurfer's segmentation method is not sensitive to gray matter atrophy. Support for this comes from the replication of age-related patterns of cortical thinning across within-study independent samples (Salat et al., 2004). Therefore, correction for intra-cranial volume was not performed.

The procedures employed by FreeSurfer have been validated against histological analysis (Rosas et al., 2002) and manual measurements (Kuperberg et al., 2003; Salat et al., 2004) and show good test-retest reliability across scanner manufacturers and field strengths (Han et al., 2006; Jovicich et al., 2009; Wonderlick et al., 2009).

2.3.3. Statistical analyses

Between-group differences in age, years of education, number of risk factors, waist circumference, triglycerides, HDL-C, systolic and diastolic BP, fasting blood glucose, and body mass index were examined either with independent-sample Student's *t*-tests (for normally distributed data as assessed with a Shapiro-Wilk test), the Wilcoxon rank-sum test with continuity correction (for non-normally distributed data), or the Welch's *t*-test (when there was a significant group difference in variance as assessed with an *F*-test). Fisher's exact tests were employed to examine group differences on categorical variables, including gender, ethnicity, and type of medication used. Statistical analyses are two-tailed with an alpha level set at $p < 0.050$ and carried out in R (Version 3.2.2) (Team, 2015).

Between-group differences in CT were examined with a general linear model (GLM) at each vertex across the whole brain surface (FreeSurfer's “mri_glmfit”). The vertex-wise and cluster-forming thresholds were set at $p < 0.050$ and resulting maps were then cluster-wise corrected for multiple comparisons with pre-computed Monte-Carlo simulations of 10,000 iterations that are provided with the FreeSurfer suite (“mri_glmfit-sim”). Cohen's *d* effect size maps were calculated by dividing the difference between the group means by the pooled standard deviation and vertices with $d > 0.5$ displayed in Fig. S.1A (in Supplements). Unstandardized effect size maps were generated simply as the group differences in CT to present the magnitude of the effects in a more intuitive metric. Vertices with CT differences between 0.1 and 0.4 mm are shown in Fig. S.1B (in Supplements). Ad-hoc independent samples Student's *t*-tests were carried out to examine average CT of the right and the left hemisphere and cortical gray and white matter volumes to provide support that observed clusters are regionally specific and not due to global structural differences between the groups. As the groups have an equal and only limited number of

Table 1
Participant characteristics in each group.

	MetS (N = 18)	Control (N = 18)	Significance tests
Age (years)	59.78 ± 12.75 (32–79)	60.50 ± 12.38 (34–79)	Student's <i>t</i> (34) = 0.17, <i>p</i> = 0.864 (<i>p</i> = 0.912) CI = -7.79 to 9.24
Gender (women/men)	6/12	4/14	Fisher's exact test <i>p</i> = 0.711 (<i>p</i> = 0.795)
Ethnicity			
African American	5	4	Fisher's exact test <i>p</i> = 0.711 (<i>p</i> = 0.795)
Asian	1	0	
White	12	14	
Education (years)	14.33 ± 1.81 (12–18)	15.44 ± 2.45 (12–20)	Student's <i>t</i> (34) = 1.54, <i>p</i> = 0.132 (<i>p</i> = 0.205) CI = -0.35 to 2.57
Number of risk factors ^a	3.67 ± 0.69 (3–5)	1.17 ± 0.86 (0–2)	Wilcoxon = 0, <i>p</i> = 0.000 (<i>p</i> = 0.000)
Waist circumference (cm)	113.00 ± 14.04 (92–141)	94.50 ± 11.31 (71–110)	Student's <i>t</i> (34) = -4.35, <i>p</i> = 0.000 (<i>p</i> = 0.000) CI = -27.13 to -9.87
Triglycerides (mg/dL) ^b	162.28 ± 69.12 (51–324)	82.44 ± 28.42 (42–132)	Welch's <i>t</i> (22.59) = -4.53, <i>p</i> = 0.000 (<i>p</i> = 0.000) CI = -116.31 to -43.36
HDL-C (mg/dL) ^c	44.82 ± 12.77 (25–76)	57.28 ± 14.05 (35–80)	Student's <i>t</i> (33) = -2.74, <i>p</i> = 0.010 (<i>p</i> = 0.027) CI = 3.20 to 21.71
Systolic BP (mm Hg)	131.50 ± 13.36 (100–161)	120.22 ± 15.59 (97–160)	Student's <i>t</i> (34) = -2.33, <i>p</i> = 0.026 (<i>p</i> = 0.055) CI = -21.11 to -1.44
Diastolic BP (mm Hg)	80.89 ± 13.51 (60–114)	77.22 ± 9.48 (52–93)	Student's <i>t</i> (34) = -0.94, <i>p</i> = 0.353 (<i>p</i> = 0.479) CI = -11.57 to 4.24
Fasting blood glucose (mg/dL) ^b	121.67 ± 48.76 (90–303)	89.83 ± 15.47 (56–117)	Welch's <i>t</i> (20.39) = -2.64, <i>p</i> = 0.016 (<i>p</i> = 0.038) CI = -56.95 to -6.17
BMI (kg/m ²) ^{b,d}	33.67 ± 5.52 (26–44)	25.06 ± 3.11 (20–31)	Welch's <i>t</i> (27.10) = -5.72, <i>p</i> = 0.000 (<i>p</i> = 0.000) CI = -11.69 to -5.52
Medication (taking)			
Triglycerides	6	2	Fisher's exact test <i>p</i> = 1.000 (<i>p</i> = 1.000)
HDL-C	0	0	
Glucose	2	0	
BP	10	5	

Continuous variables are expressed as mean ± standard deviation and (range). MetS = Metabolic Syndrome; cm = centimeter; mg/dL = milligrams per deciliter; HDL-C = high-density lipoprotein cholesterol; BP = blood pressure; mm Hg = millimeters of mercury; BMI = body mass index provided for comparison with other studies. CI = 95% confidence interval. Bolded *p*-values indicate significant results. False discovery rate-corrected *p*-values are indicated in parentheses.

^a Data not normally distributed.

^b Unequal between-sample variance.

^c Missing data for one participant in the MetS group.

^d Missing data for one participant in the control group.

individuals scanned at a different location (i.e., 3/18 in each group were scanned at the VA) no additional analysis including scan location as a covariate was carried out. Prior studies have shown minimal effects of different MRI instrument parameters on CT measurements (Han et al., 2006; Wonderlick et al., 2009).

Follow-up multivariate PLS analyses were used to investigate how individual MetS risk factors relate to average CT in GLM-derived clusters that are associated with MetS (“Behavioral PLS” from the PLS toolbox version 6.15.1 run in MATLAB version R2015b; <https://www.rotman-baycrest.on.ca/pls>). PLS analyses are well suited for highly correlated dependent variables, which might be expected when the patterns of CT are similar across clusters (McIntosh and Lobaugh, 2004). Data from the full sample with complete risk factor measurements (i.e., 53/55 participants) were entered as continuous measures. Systolic and diastolic BP were both included, yielding six MetS risk factor components. In this data-driven analysis, the correlation between CT in the GLM-derived clusters and individual MetS risk factor components was computed and singular value decomposition was performed on this correlation matrix to determine orthogonal latent variables that maximize the covariance between these two sets of data (McIntosh and Lobaugh, 2004). The statistical significance (set at *p* < 0.050) of latent variables was computed with permutation tests (10,000 samples without replacement), producing a sampling distribution of singular values under the null hypothesis that the effects associated with the latent variable are not different from random noise. The use of permutations allows interpretation similar to a random-effects model. The reliability of CT clusters contributing to a given significant latent variable was determined via bootstrap resampling (10,000 times with replacement) of the associated saliences to estimate their standard error. Confidence intervals (95%) for the correlation between latent variables and MetS risk factors were

derived from the bootstrap distribution. Bootstrap ratios, computed as salience-to-salience standard error (i.e., across the bootstrap samples), can be treated as approximately equivalent to *z*-scores (McIntosh and Lobaugh, 2004). CT clusters were considered reliable contributors if bootstrap ratios were ≥ 2.0 (1.96 rounded), a value frequently used in the PLS literature (Krishnan et al., 2011; Palombo et al., 2016; Tchistiakova et al., 2016). The use of permutation and bootstrap techniques make this analysis approach statistically robust. Since permutations are performed on the CT and MetS risk factor matrices simultaneously and bootstrapping is performed to assess the reliability of effects (i.e., not representing a statistical test), multiple testing correction is not necessary (McIntosh and Lobaugh, 2004; Tchistiakova et al., 2016). A control PLS analysis was performed, including the participant's age as a predictor in the model, as MetS risk factors as well as CT in these brain regions have been associated with this variable. The goal was to determine whether age could be dissociated as a driving factor to the observed correlation pattern.

The *p*-values of all significance tests (except for the GLM) implemented in this study were adjusted using the false discovery rate (FDR; “p.adjust” included in R's “stats” package) and presented following the original *p*-values in Table 1 or in the text.

3. Results

3.1. Participants

In the MetS group, eight (44%) participants met thresholds for three risk factors, seven (39%) met thresholds for four, and two (11%) participants met thresholds for all five risk factors (note that one participant did not have the HDL-C measure, and therefore, an exact risk

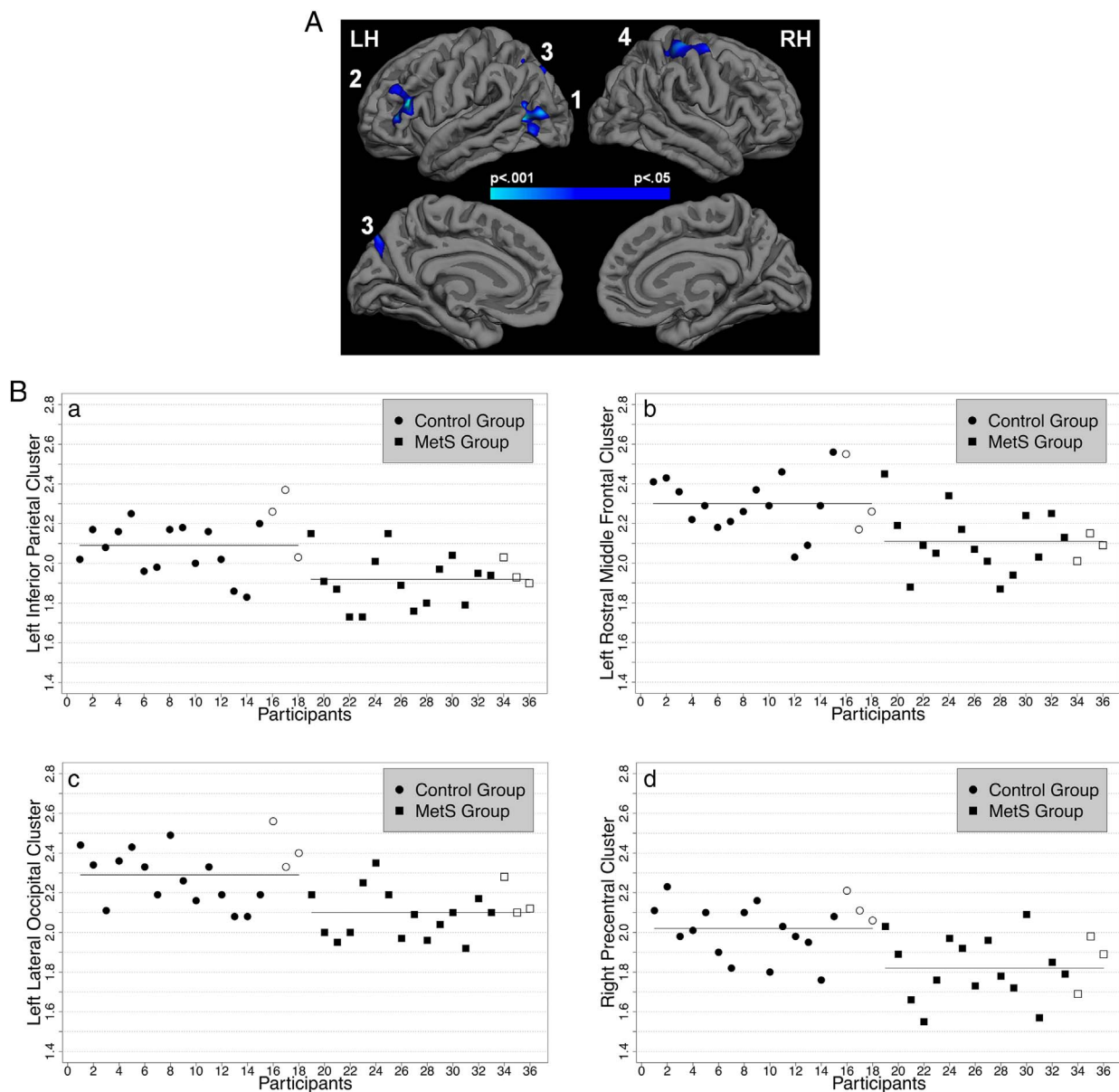


Fig. 1. A. Significantly reduced cortical thickness (CT) in the Metabolic Syndrome (MetS) group in left 1) inferior parietal, 2) rostral middle frontal, 3) lateral occipital regions, and right 4) precentral regions relative to the control group as assessed with a whole-brain general linear model (GLM). The significance map is presented on the pial surface of an average brain (“fsaverage”, provided by FreeSurfer) with dark gray representing sulci and light gray representing gyri. The color scale indicates *p*-values (thresholded at vertex- and cluster-wise $p < 0.050$). Results were multiple comparison corrected with Monte-Carlo simulations. See Table 2 for more information. B. Average CT in the GLM-derived clusters. Horizontal lines indicate group means. Symbols without color filling indicate participants scanned at the Veterans Administration Boston Healthcare System (VA).

factor count could not be calculated). Waist circumference was most often ($N = 16/89\%$) met, followed by BP ($N = 15/83\%$), triglycerides ($N = 14/78\%$), glucose ($N = 12/67\%$), and HDL-C ($N = 9/50\%$). In the control group, five (28%) participants did not meet any of the risk factor thresholds, five (28%) met one, and eight (44%) participants met thresholds for two risk factors. BP was the most common risk factor ($N = 8/44\%$) observed, followed by waist circumference ($N = 6/33\%$), glucose ($N = 4/22\%$), triglycerides ($N = 2/11\%$), and HDL-C ($N = 1/6\%$). Consistent with prior literature and in expected directions, the groups significantly differed in the number of risk factors, waist circumference, HDL-C, triglycerides, glucose, and body mass index (the latter only provided to enable comparison with other studies). They also significantly differed on systolic but not diastolic BP. There were no significant group differences in the use of medication for BP, dyslipidemia, and hyperglycemia. The groups did not significantly differ in age, gender distribution, or years of education (Table 1).

3.2. Imaging

The primary whole-brain between-group GLM analysis revealed three clusters in the left and one cluster in the right hemisphere that survived multiple comparison correction. The MetS group demonstrated significantly reduced CT relative to the control group in 1) a left inferior parietal cluster extending into middle temporal regions, 2) a left rostral middle frontal cluster extending into inferior frontal regions, 3) a left lateral occipital cluster, and 4) a cluster in right precentral gyrus that spans postcentral and superior parietal regions (Fig. 1A and B and Table 2). These results appear to be regionally specific and not due to global structural differences as the groups did not significantly differ in average CT in the left ($t(34) = 1.71, p = 0.096$ (FDR-adjusted $p = 0.182$), confidence interval (CI) = -0.01 – 0.14) nor right ($t(34) = 1.51, p = 0.140$ (FDR-adjusted $p = 0.205$), CI = -0.02 – 0.13) hemisphere and neither in gray ($t(34) = 1.57, p = 0.127$ (FDR-adjusted

Table 2
Summary information on clusters that survived multiple comparison correction.

Cortical region	Average cortical thickness (mm) ^a		Number of vertices	Cluster size (mm ²)	Maximum <i>t</i> -value	Talairach ^b (x y z)
	Control (N = 18)	MetS (N = 18)				
<i>LH</i>						
Inferior parietal (1)	2.09 ± 0.14	1.92 ± 0.13	2245	1311.27	− 4.69	− 31.9 − 73.1 22.8
Rostral middle frontal (2)	2.30 ± 0.15	2.11 ± 0.15	1286	871.28	− 3.66	− 40.2 26.4 15.2
Lateral occipital (3)	2.29 ± 0.14	2.10 ± 0.12	1481	823.45	− 3.25	− 41.4 − 63.8 4.7
<i>RH</i>						
Precentral (4)	2.02 ± 0.14	1.82 ± 0.15	3449	1436.09	− 3.50	34.4 − 20.2 49.0

LH = left hemisphere and RH = right hemisphere. Numbers next to cortical regions indicate clusters in Fig. 1A. Anatomical description reflects FreeSurfer naming conventions.

^a Expressed in mean ± standard deviation.

^b Coordinates of maximum *t*-value.

$p = 0.205$), CI = − 7175.09–55,387.80) nor white ($t(34) = 0.87$, $p = 0.391$ (FDR-adjusted $p = 0.495$), CI = − 25,849.65–64,537.48) matter volumes. Furthermore, CT averages of the three participants per group scanned at the VA fell within two standard deviations of their respective group averages (shape-coded in Fig. 1B). There were no regions in which the MetS group had significantly thicker gray matter relative to the control group.

As expected, the standardized (i.e., Cohen's d) and unstandardized (i.e., CT group differences) effect size maps encompass the GLM clusters but also reveal strong effects bilaterally in portions of frontal, temporal, parietal, and occipital regions (Supplement Fig. S.1A and B). Furthermore, the maps illustrate a predominance of reduced CT in the MetS group relative to the control group. In contrast to the GLM results, effect sizes indicating greater CT in the MetS group were also seen in a few regions, for example in cingulate cortex or in bilateral anterior fusiform gyrus although the latter did not emerge in the Cohen's d maps at the chosen threshold. Overall, the effect size maps suggest larger and more distributed regions of robust effect magnitude wherein the groups might differ in CT compared to the GLM results. The relatively weaker outcome from the GLM may be due to the small sample size. In addition, the CT differences between the groups > 0.1 mm (with largest values of 0.4 mm) in the present study are sizable and well in-line with previous literature in MetS (Song et al., 2015) and other populations (Brundel et al., 2010; Hassenstab et al., 2012; Preul et al., 2005; Salat et al., 2004; Seo et al., 2012).

FDR-correction across p -values of all statistical tests (except the GLM) carried out in this study did not change the results except for the group difference in systolic BP, which was reduced to trend-level after correction (Table 1).

3.3. Partial least squares correlation

The follow-up PLS analysis revealed one significant latent variable ($p < 0.001$; FDR-adjusted $p = 0.003$) that accounted for 97% of the covariance between average CT in the GLM-derived clusters and MetS risk factor components (for sample characteristics see Table 3). CT saliences, representing the strength of the CT cluster contribution, were reliably associated with the latent variable as indicated by bootstrap ratios of 2.99 for the left inferior parietal, 3.05 for the left rostral middle frontal, 3.97 for the left lateral occipital, and 3.09 for the right precentral cluster. This analysis revealed that these brain regions were associated with a subset of risk factors, shown in Fig. 2A, which illustrates the correlation between individual risk factor components and the latent variable. The correlations are mostly in expected directions, with larger values for waist circumference, triglycerides, and glucose being associated with reduced CT. The relationship should be opposite for HDL-C, wherein lower values are indicative of poorer health, which is indeed observed. Interestingly, the correlations for the two BP measures differed in their relationship to gray matter integrity; higher systolic BP was associated (although only weakly) with reduced CT

while higher diastolic BP was associated with greater CT. Of the six risk factor components included in the model, waist circumference, triglycerides, HDL-C, glucose, and diastolic BP were significant contributors to the latent variable as indicated by confidence intervals (represented by error bars in Fig. 2A) not crossing the horizontal line (i.e., excluding zero). None of the significantly associated risk factor indices contributed separately relative to the others as indicated by overlapping confidence intervals (inverting HDL-C and diastolic BP to match the positive association between elevated levels on other variables and reduced CT was used to confirm the non-overlap). Therefore, waist circumference, HDL-C, triglycerides, glucose, and diastolic BP were interpreted as common contributors to the latent variable. Fig. 2B shows scatterplots illustrating the relationships between the significant latent variable and raw values of the six risk factor components. Results did not change when age was included in the model (Fig. 2A). One significant latent variable ($p < 0.001$; FDR-adjusted $p = 0.003$) accounted for 97% of the covariance between the sets of data. Bootstrap ratios were 3.17 for the left inferior parietal, 2.98 for the left rostral middle frontal, 4.24 for the left lateral occipital, and 3.27 for the right precentral cluster. As before, waist circumference, triglycerides, HDL-C, glucose, and diastolic BP remained significant contributors to this association pattern.

4. Discussion

The main findings of the current study were twofold. First, we observed significantly reduced CT in the MetS group in both hemispheres: in left rostral middle frontal, inferior parietal, and lateral occipital and right precentral regions, providing support for the notion that MetS may have negative effects on gray matter integrity. Second, a follow-up PLS analysis revealed that, of the six MetS risk factor components (BP was stratified into systolic and diastolic BP), waist circumference, triglycerides, HDL-C, glucose, and diastolic BP were significantly associated with CT in those clusters, whereas systolic BP and age were not associated. These results provide a novel link between a particular MetS risk factor profile and localized alterations in gray matter integrity, suggesting that there may be a specific risk factor combination that increases vulnerability for damage to aspects of brain structure. Our results can direct future investigations examining underlying pathophysiological mechanisms by which MetS risk factors may impact brain health.

Reduced CT in the right precentral cluster in the MetS group observed here closely approximates, spatially, the superior parietal cluster reported in a prior study in a MetS cohort, although we did not detect their findings in the left hemisphere (Song et al., 2015) or in medial temporal lobe structures described in another study (McIntosh et al., 2017). However, we identified reduced CT in additional regions in left hemisphere frontal and occipital cortices. The effect size maps presented here show distributed patterns of moderate to large effects, replicating and extending the observations of reduced CT in the MetS

Table 3
Characteristics of the cohort (N = 53) included in the partial least squares correlation analyses.

Age (years)	59.85 ± 13.82 (30–85)
Gender (women/men)	20/33
Ethnicity	
African American	13
American Indian	1
Asian	1
White	38
Education (years)	15.13 ± 2.35 (11–20)
Number of risk factors	1.98 ± 1.39 (0–5)
Waist circumference (cm)	99.21 ± 16.36 (70–141)
Triglycerides (mg/dL)	108.62 ± 57.52 (42–324)
HDL-C (mg/dL)	54.72 ± 16.04 (25–100)
Systolic BP (mm Hg)	123.09 ± 16.24 (87–160)
Diastolic BP (mm Hg)	76.43 ± 11.21 (52–100)
Fasting blood glucose (mg/dL)	96.28 ± 18.80 (55–160)
Body Mass Index (kg/m ²) ^a	28.49 ± 6.06 (20–45)
Risk factor prevalence:	
Blood pressure	31
Waist circumference	26
Triglycerides	20
Fasting blood glucose	17
HDL-C	11
Inferior parietal (1)	2.00 ± 0.16
Rostral middle frontal (2)	2.20 ± 0.16
Lateral occipital (3)	2.19 ± 0.15
Precentral (4)	1.93 ± 0.17
Mediation (taking)	
Triglycerides	13
HDL-C	0
Glucose	2
Blood pressure	21

Continuous variables are expressed as mean ± standard deviation and (range). cm = centimeter; mg/dL = milligrams per deciliter; HDL-C = high-density lipoprotein cholesterol; mm Hg = millimeters of mercury. Note: two participants from the full study sample (i.e., N = 55) were excluded due to either missing HDL-C or waist circumference measurements.

^a Missing for one participant; body mass index is provided for comparison with other studies.

groups in those prior studies. Interestingly, they also exhibit regions of greater CT in the MetS group relative to the control group. It remains to be seen if and in which manner risk factors may relate to this opposite pattern, although cholesterol (Leritz et al., 2011), lipid factors (Krishnadas et al., 2013), and adiposity (Saute et al., 2016) may play a role considering their linking to greater CT in community samples. The differential findings between the present and prior investigations may be due to particular cohort characteristics reflecting variations in MetS severity across studies. Our MetS group has larger waist circumference and demonstrates higher levels of glucose and triglycerides in comparison to Song et al. (2015) and a greater number of risk factors but smaller waist circumference and lower systolic BP (glucose and lipid data were not presented) compared to McIntosh et al. (2017). It is conceivable that our results might represent brain regions that are susceptible to greater MetS-related pathology. A previous study reported an association between greater MetS severity scores and reduced CT in an overlapping region in left inferior parietal cortex in U.S. military veterans (Wolf et al., 2016). As such, the present findings partly support, and putatively extend, the currently sparse literature delineating MetS effects on gray matter structure.

Individual risk factors have been linked to alterations in gray matter thickness in similar regions as observed here. Hypertension has been associated with reduced CT in frontal, temporal, and parietal cortices in older community samples (Leritz et al., 2011; Vuorinen et al., 2013) and participants with cognitive impairment (Seo et al., 2012), with frontal and parietal regions approximating or overlapping with the present results. Measures of obesity have shown associations with reduced CT in frontal and parietal cortices (Hassenstab et al., 2012; Veit et al., 2014) and in inferior parietal cortex (Veit et al., 2014), the latter

overlapping with our result. However, some studies did not find effects related to body mass index (Krishnadas et al., 2013; Vuorinen et al., 2013), while others have identified greater CT in relation to visceral fat in adolescents in portions of frontal and superior parietal cortices comparable to the present study (Saute et al., 2016) and in posterior cingulate cortex in middle-aged adults (Kaur et al., 2015a). Diabetes has been related to decreased CT in frontal, temporal, and parietal cortices (Seo et al., 2012; Tchistiakova et al., 2014; van Velsen et al., 2013) but fasting blood glucose, as part of a factor score, was not related to CT in a community sample (Leritz et al., 2011). Discrepancies across studies may, in part, arise from the particular measure collected to index metabolic and vascular risk factors, and how these measures were included in analyses. For example, relationships between higher levels of HDL-C and reduced CT were reported in the occipital lobe (van Velsen et al., 2013), while factor scores that included HDL-C did not show significant associations (Krishnadas et al., 2013; Leritz et al., 2011). In contrast, levels of serum total cholesterol (Vuorinen et al., 2013) were not related to CT, while factor scores including total cholesterol, low-density lipoprotein cholesterol, or very low-density lipoprotein cholesterol were related to increased CT, spanning parts of the cerebral cortex that include regions reported here (Krishnadas et al., 2013; Leritz et al., 2011). Similar mixed results were reported for factors including triglyceride levels (Krishnadas et al., 2013; Leritz et al., 2011) and studies employing different indices of obesity (Kaur et al., 2015a; Krishnadas et al., 2013; Saute et al., 2016). Including both BP indices jointly as a factor showed a negative relationship to CT (Leritz et al., 2011), yet when examined separately, higher diastolic BP was affiliated with greater global and frontal lobe CT while no effects were identified for systolic BP (van Velsen et al., 2013). This observation is in agreement with our findings. Divergent associations of metabolic factors have been reported in white matter microstructure as well and allude to competing disease mechanisms (Verstynen et al., 2013). The mechanisms underlying a pathophysiological impact of MetS on cortical gray matter are likely complex. Therefore, a complementary approach to studying MetS risk factors as components of factor scores or in isolation is to examine their contributions in context of each other.

To address this issue, a follow-up multivariate PLS analysis, incorporating continuous physiological raw data, was used to identify association patterns between MetS risk factors and CT. Of the six MetS risk factor components, elevations in waist circumference, triglycerides, glucose, lower levels of HDL-C, and higher diastolic BP demonstrated a significant relationship to CT in brain regions in which the MetS group had significantly reduced gray matter thickness relative to the control group. These observations are in line with the currently accepted definition of MetS comprising these risk factors (Grundy, 2005) and fit with previous factor analyses of metabolic and vascular variables (Gray et al., 1998; Hanley et al., 2002; Leritz et al., 2011; Meigs, 2000; Meigs et al., 1997; Sakkinen et al., 2000). In particular, a confirmatory factor analysis using a hierarchical four-factor model revealed that insulin resistance (including a fasting glucose measure) and obesity factors showed the strongest associations with a higher-order MetS factor, followed by a moderate association for a lipid factor, while a BP factor was least related (Shen et al., 2003). While hypertension has been linked to reduced CT in brain regions partly overlapping with the results reported here (Leritz et al., 2011; Seo et al., 2012; Vuorinen et al., 2013), the relationship of BP to other MetS risk factors appears to be most tenuous as it frequently forms a unique component in factor analyses (Meigs, 2000), alluding to secondary or separate pathology. Here, we observed a positive affiliation between diastolic BP and CT, which is in accord with prior literature (van Velsen et al., 2013). Higher diastolic BP has been associated with increased perfusion in the right temporal cortex in women (Waldstein et al., 2010). Together, this suggests that perhaps there is an optimal level of this particular risk factor that can be beneficial to brain health, but the implications for brain health await further examination. In contrast, systolic BP did not emerge as a contributor to the relationship between MetS risk factors

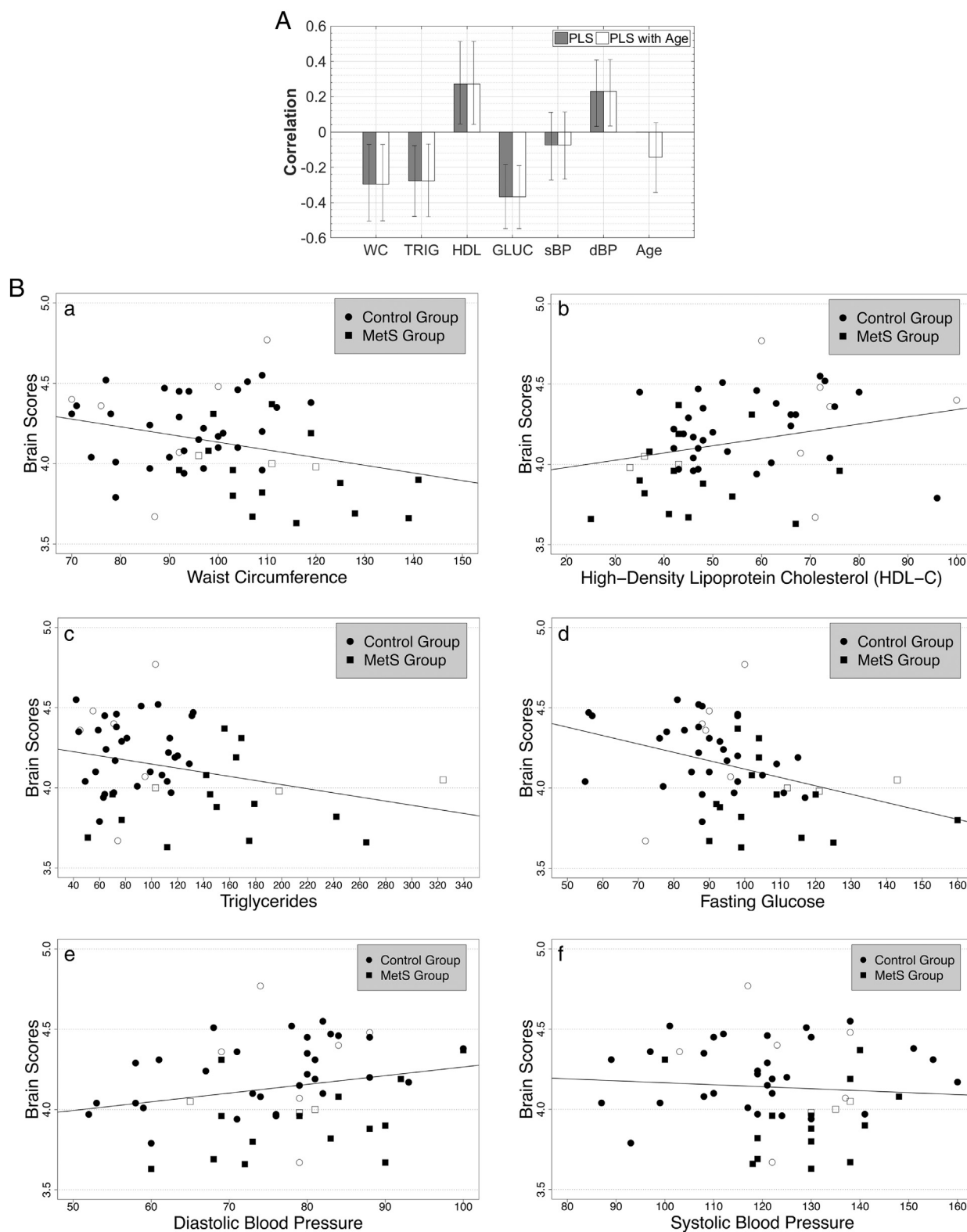


Fig. 2. A. Significant latent variable from the partial least squares correlation (PLS) analysis that maximizes the covariance between cortical thickness (CT) in the clusters derived from the whole-brain general linear model (GLM; Fig. 1A) and individual risk factors for Metabolic Syndrome (MetS). Shown are the correlations between “brain scores” (representing how well clusters contribute to the overall latent variable pattern) and raw values of MetS risk factors, as indicated with gray bars, and when age was included in the model, with white bars. WC = waist circumference; TRIG = triglycerides; HDL = high-density lipoprotein cholesterol; GLUC = fasting blood glucose; s = systolic and d = diastolic BP = blood pressure. Error bars represent 95% confidence intervals (CI) and indicate the significance of the relationship between the latent variable and MetS risk factor and age variables. Risk factors with error bars crossing the horizontal axis are not significant contributors to the latent variable. Of note is the minimal change in correlation magnitude and CI size between the two PLS analyses. See Table 3 for sample characteristics. B. Raw values of MetS risk factor components plotted against brain scores. Group membership of participants is indicated to provide additional information; symbols without color filling indicate participants scanned at the Veterans Administration Boston Healthcare System (VA). Note: high-density lipoprotein cholesterol is expected to show a positive relationship as lower values on this variable indicate worse health.

and CT. This is consistent with a recent study which found that systolic BP was only associated with right medial temporal lobe structures in middle-aged adults but not when used as a covariate examining CT differences between a MetS and a control group (McIntosh et al., 2017). These findings indicate that systolic BP by itself was unlikely to underlie CT group differences in right medial temporal lobe, a conclusion which we here extend to other MetS-related cortical regions. Alternatively, systolic BP may have more pronounced associations in other parts of the cerebral cortex (see Leritz et al., 2011) wherein group differences were not detected or the brain regions described here might show effects stemming from obesity, hyperglycemia, dyslipidemia, and diastolic BP earlier than from systolic BP. Characteristics of the two BP indices, such as high or low levels or the age at which alterations in BP levels appeared, may determine the nature of their influence on CT (van Velsen et al., 2013; Vuorinen et al., 2013). Thus, examining systolic and diastolic BP separately may provide a more nuanced understanding of the relationship between BP and CT. Furthermore, the control PLS analysis indicated that age was not associated with this pattern, suggesting that the contributions of these metabolic risk factors exceed potential effects of age. Although aging has been implicated in reduced CT (Fjell et al., 2009; Salat et al., 2004) and has accounted for associations between hypertension and CT (Alosco et al., 2014), it may be that the combination of obesity, hyperglycemia, dyslipidemia, and diastolic BP produces more substantial changes in regional brain morphology compared to age. Overall, results from the present approach of simultaneously incorporating MetS risk factors in the analysis links previously identified chief pathogenic factors (i.e., obesity, hyperglycemia, dyslipidemia, and to a lesser degree, hypertension) to alterations in gray matter integrity.

There are several potential mechanisms by which obesity, hyperglycemia, dyslipidemia, and diastolic BP may affect gray matter integrity. Association between MetS, obesity, and inflammation are well established (Aronson et al., 2004; Eckel et al., 2005; Libby et al., 2002). Inflammatory markers were shown to mediate the relationship between reduced CT and a greater number of MetS risk factors (Kaur et al., 2015b) and to differ significantly between lean relative to overweight/obese participants who comprised a sample where indices of obesity were associated with reduced CT in similar left inferior parietal cortex regions reported here (Veit et al., 2014). Inflammation, obesity, and insulin disturbances have been linked to vascular damage via mechanisms affecting the layers of vessel walls, such as the endothelium (Libby et al., 2002; Lind, 2008; Tesaro and Cardillo, 2011). Vasodilation, including endothelium-dependent vasodilation, was impaired in participants with MetS, and measures of waist circumference, serum triglycerides, blood glucose, and diastolic BP were identified as significant factors in these vascular alterations (Lind, 2008). The risk factor combination observed here is in alignment with these findings. Pathophysiologically, potential underlying mechanisms may be related to impaired vascular integrity resulting in reduced cerebral blood flow and perfusion, and consequentially, in poor oxygenation and shrinking of previously healthy tissue (Hoscheidt et al., 2017). Reduced cerebral blood flow has been documented in participants with MetS (Birdsill et al., 2013) and in association with individual risk factors, including waist circumference, triglycerides, glucose, and systolic BP (Birdsill et al., 2013; Jennings et al., 2013). Indeed, reduced cerebrovascular reactivity was observed in a left lateral occipital cluster, overlapping with the cluster reported here, in participants with type 2 diabetes mellitus and hypertension relative to a hypertension-only group (Tchistiakova et al., 2014). Furthermore, obesity, hyperglycemia, and dyslipidemia have been identified in the development of atherosclerosis (Libby et al., 2002) and MetS has been associated with cerebrovascular, but not peripheral, atherosclerosis, even after adjusting for a variety of cardiovascular risk factors and hemostatic and inflammatory markers (Wild et al., 2009). Consequences of vascular disturbances on brain structure are likely multifaceted and may underlie deteriorations in brain structure. Ischemic stroke (Maruyama et al., 2009) and previous

ischemic (Park and Kwon, 2008) and white matter (Bokura et al., 2008) lesions have been associated with hyperglycemia and dyslipidemia in MetS cohorts. Future efforts might examine whether the presently observed risk factor profile shows similar relationships with white matter integrity.

The present results should be interpreted with the following limitations in mind. The cross-sectional design does not allow causal inferences of MetS on CT. Prospective cohort studies designed to investigate brain changes over time would be ideal to examine progressive and reciprocal disease mechanisms that may form a particular MetS profile. Other measures, such as markers of inflammation, should be included to examine the stability and specificity of the risk factor combination comprising obesity, hyperglycemia, dyslipidemia, and diastolic BP to patterns of CT alterations in MetS. While the PLS analysis allows interpretation similar to a random-effects model, enabling preliminary generalizability to a predominantly male Caucasian demographic, different risk profiles may emerge for other ethnic groups (Aguilar et al., 2015; Ervin, 2009; Ford et al., 2002) and is an important direction for future research.

5. Conclusion

In summary, we report reductions in CT in association with MetS, consistent with prior findings, suggesting that MetS may have a regionally specific effect on gray matter. We also observed a risk factor profile that reflects extensive literature delineating obesity, hyperglycemia, dyslipidemia, and diastolic BP as core elements of MetS, and present the novel finding of an association pattern between this risk factor profile and gray matter integrity in brain regions linked to MetS. The present approach may allow for improved sensitivity to further characterize pathophysiological processes underlying MetS, and in that way, facilitating targeted intervention and prevention to counter adverse consequences such as increased morbidity and mortality, including cardiovascular disease, type 2 diabetes mellitus, and cognitive decline (Grundey, 2007, 2008; Yaffe et al., 2004; Yates et al., 2012).

Supplementary data to this article can be found online at <https://doi.org/10.1016/j.nicl.2017.09.022>.

Acknowledgements

Funding: This work was supported by the National Institute of Neurologic Disorders and Stroke (grant number R01NS086882), the National Institute of Nursing Research (grant number R01NR01827), and by a Medical Research Service VA Merit Review Award to Regina McGlinchey.

References

- Aguilar, M., Bhuket, T., Torres, S., Liu, B., Wong, R.J., 2015. Prevalence of the metabolic syndrome in the United States, 2003–2012. *JAMA* 313 (19), 1973–1974.
- Alosco, M.L., Gunstad, J., Xu, X., Clark, U.S., Labbe, D.R., Riskin-Jones, H.H., ... Poppas, A., 2014. The impact of hypertension on cerebral perfusion and cortical thickness in older adults. *J. Am. Soc. Hypertens.* 8 (8), 561–570.
- Aronson, D., Bartha, P., Zinder, O., Kerner, A., Markiewicz, W., Avizohar, O., ... Levy, Y., 2004. Obesity is the major determinant of elevated C-reactive protein in subjects with the metabolic syndrome. *Int. J. Obes.* 28 (5), 674–679.
- Beltrán-Sánchez, H., Harhay, M.O., Harhay, M.M., McElligott, S., 2013. Prevalence and trends of metabolic syndrome in the adult US population, 1999–2010. *J. Am. Coll. Cardiol.* 62 (8), 697–703.
- Birdsill, A.C., Carlsson, C.M., Willette, A.A., Okonkwo, O.C., Johnson, S.C., Xu, G., ... Jonaitis, E.M., 2013. Low cerebral blood flow is associated with lower memory function in metabolic syndrome. *Obesity* 21 (7), 1313–1320.
- Bokura, H., Yamaguchi, S., Iijima, K., Nagai, A., Oguro, H., 2008. Metabolic syndrome is associated with silent ischemic brain lesions. *Stroke* 39 (5), 1607–1609.
- Brundel, M., van den Heuvel, M., de Bresser, J., Kappelle, L.J., Biessels, G.J., Group, U. D. E. S., 2010. Cerebral cortical thickness in patients with type 2 diabetes. *J. Neurol. Sci.* 299 (1), 126–130.
- Dale, A.M., Sereno, M.I., 1993. Improved localization of cortical activity by combining EEG and MEG with MRI cortical surface reconstruction: a linear approach. *J. Cogn. Neurosci.* 5 (2), 162–176.
- Dale, A.M., Fischl, B., Sereno, M.I., 1999. Cortical surface-based analysis: I. Segmentation

- and surface reconstruction. *NeuroImage* 9 (2), 179–194.
- Destrieux, C., Fischl, B., Dale, A., Halgren, E., 2010. Automatic parcellation of human cortical gyri and sulci using standard anatomical nomenclature. *NeuroImage* 53 (1), 1–15.
- Eckel, R.H., Grundy, S.M., Zimmet, P.Z., 2005. The metabolic syndrome. *Lancet* 365 (9468), 1415–1428.
- Ervin, R.B., 2009. Prevalence of metabolic syndrome among adults 20 years of age and over, by sex, age, race and ethnicity, and body mass index: United States. *Natl. Health Stat. Rep.* 13, 1–8.
- Fischl, B., 2012. FreeSurfer. *NeuroImage* 62 (2), 774–781.
- Fischl, B., Dale, A.M., 2000. Measuring the thickness of the human cerebral cortex from magnetic resonance images. *Proc. Natl. Acad. Sci.* 97 (20), 11050–11055.
- Fischl, B., Sereno, M.I., Dale, A.M., 1999a. Cortical surface-based analysis: II: inflation, flattening, and a surface-based coordinate system. *NeuroImage* 9 (2), 195–207.
- Fischl, B., Sereno, M.I., Tootell, R.B., Dale, A.M., 1999b. High-resolution intersubject averaging and a coordinate system for the cortical surface. *Hum. Brain Mapp.* 8 (4), 272–284.
- Fischl, B., Liu, A., Dale, A.M., 2001. Automated manifold surgery: constructing geometrically accurate and topologically correct models of the human cerebral cortex. *IEEE Trans. Med. Imaging* 20 (1), 70–80.
- Fischl, B., Salat, D.H., Busa, E., Albert, M., Dieterich, M., Haselgrove, C., ... Klaveness, S., 2002. Whole brain segmentation: automated labeling of neuroanatomical structures in the human brain. *Neuron* 33 (3), 341–355.
- Fischl, B., Salat, D.H., van der Kouwe, A.J., Makris, N., Ségonne, F., Quinn, B.T., Dale, A.M., 2004a. Sequence-independent segmentation of magnetic resonance images. *NeuroImage* 23, S69–S84.
- Fischl, B., Van Der Kouwe, A., Destrieux, C., Halgren, E., Ségonne, F., Salat, D.H., ... Kennedy, D., 2004b. Automatically parcellating the human cerebral cortex. *Cereb. Cortex* 14 (1), 11–22.
- Fjell, A.M., Westlye, L.T., Amlie, I., Espeseth, T., Reinvang, I., Raz, N., ... Fischl, B., 2009. High consistency of regional cortical thinning in aging across multiple samples. *Cereb. Cortex*, bhn232.
- Ford, E.S., Giles, W.H., Dietz, W.H., 2002. Prevalence of the metabolic syndrome among US adults: findings from the third National Health and Nutrition Examination Survey. *JAMA* 287 (3), 356–359.
- Friedman, J.I., Tang, C.Y., de Haas, H.J., Changchien, L., Goliasch, G., Dabas, P., ... Narula, J., 2014. Brain imaging changes associated with risk factors for cardiovascular and cerebrovascular disease in asymptomatic patients. *J. Am. Coll. Cardiol. Img.* 7 (10), 1039–1053.
- Gray, R.S., Fabsitz, R.R., Cowan, L.D., Lee, E.T., Howard, B.V., Savage, P.J., 1998. Risk factor clustering in the insulin resistance syndrome The Strong Heart Study. *Am. J. Epidemiol.* 148 (9), 869–878.
- Grundy, S.M., 2005. Metabolic syndrome scientific statement by the American Heart Association and the National Heart, Lung, and Blood Institute. *Arterioscler. Thromb. Vasc. Biol.* 25 (11), 2243–2244.
- Grundy, S.M., 2007. Metabolic syndrome: a multiplex cardiovascular risk factor. *J. Clin. Endocrinol. Metab.* 92 (2), 399–404.
- Grundy, S.M., 2008. Metabolic syndrome pandemic. *Arterioscler. Thromb. Vasc. Biol.* 28 (4), 629–636.
- Han, X., Jovicich, J., Salat, D., van der Kouwe, A., Quinn, B., Czanner, S., ... Killiany, R., 2006. Reliability of MRI-derived measurements of human cerebral cortical thickness: the effects of field strength, scanner upgrade and manufacturer. *NeuroImage* 32 (1), 180–194.
- Hanley, A.J., Karter, A.J., Festa, A., D'Agostino, R., Wagenknecht, L.E., Savage, P., ... Haffner, S., 2002. Factor analysis of metabolic syndrome using directly measured insulin sensitivity the insulin resistance atherosclerosis study. *Diabetes* 51 (8), 2642–2647.
- Hanson, R.L., Imperatore, G., Bennett, P.H., Knowler, W.C., 2002. Components of the “metabolic syndrome” and incidence of type 2 diabetes. *Diabetes* 51 (10), 3120–3127.
- Hassenstab, J.J., Sweet, L.H., Del Parigi, A., McCaffery, J.M., Haley, A.P., Demos, K.E., ... Wing, R.R., 2012. Cortical thickness of the cognitive control network in obesity and successful weight loss maintenance: a preliminary MRI study. *Psychiatry Res. Neuroimaging* 202 (1), 77–79.
- Hoscheidt, S.M., Kellawan, J.M., Berman, S.E., Rivera-Rivera, L.A., Krause, R.A., Oh, J.M., ... Carlsson, C.M., 2017. Insulin resistance is associated with lower arterial blood flow and reduced cortical perfusion in cognitively asymptomatic middle-aged adults. *J. Cereb. Blood Flow Metab.* 37 (6), 2249–2261.
- Jacobs, H.I., Clerx, L., Gronenschild, E.H., Aalten, P., Verhey, F.R., 2014. White matter hyperintensities are positively associated with cortical thickness in Alzheimer's disease. *J. Alzheimers Dis.* 39 (2), 409–422.
- Jennings, J.R., Heim, A.F., Kuan, D.C.-H., Gianaros, P.J., Muldoon, M.F., Manuck, S.B., 2013. Use of total cerebral blood flow as an imaging biomarker of known cardiovascular risks. *Stroke* 44 (9), 2480–2485.
- Jovicich, J., Czanner, S., Han, X., Salat, D., van der Kouwe, A., Quinn, B., ... Blacker, D., 2009. MRI-derived measurements of human subcortical, ventricular and intracranial brain volumes: reliability effects of scan sessions, acquisition sequences, data analyses, scanner upgrade, scanner vendors and field strengths. *NeuroImage* 46 (1), 177–192.
- Kaur, S.S., Gonzales, M.M., Strasser, B., Pasha, E., McNeely, J., Tanaka, H., Haley, A.P., 2015a. Central adiposity and cortical thickness in midlife. *Psychosom. Med.* 77 (6), 671–678.
- Kaur, S.S., Gonzales, M.M., Eagan, D.E., Goudarzi, K., Tanaka, H., Haley, A.P., 2015b. Inflammation as a mediator of the relationship between cortical thickness and metabolic syndrome. *Brain Imaging Behav.* 9 (4), 737–743.
- Krishnadas, R., McLean, J., Batty, D.G., Burns, H., Deans, K.A., Ford, I., ... Millar, K., 2013. Cardio-metabolic risk factors and cortical thickness in a neurologically healthy male population: results from the psychological, social and biological determinants of ill health (pSoBid) study. *NeuroImage Clin.* 2, 646–657.
- Krishnan, A., Williams, L.J., McIntosh, A.R., Abdi, H., 2011. Partial Least Squares (PLS) methods for neuroimaging: a tutorial and review. *NeuroImage* 56 (2), 455–475.
- Kuperberg, G.R., Broome, M.R., McGuire, P.K., David, A.S., Eddy, M., Ozawa, F., ... van der Kouwe, A.J., 2003. Regionally localized thinning of the cerebral cortex in schizophrenia. *Arch. Gen. Psychiatry* 60 (9), 878–888.
- Leritz, E.C., Salat, D.H., Williams, V.J., Schnyer, D.M., Rudolph, J.L., Lipsitz, L., ... Milberg, W.P., 2011. Thickness of the human cerebral cortex is associated with metrics of cerebrovascular health in a normative sample of community dwelling older adults. *NeuroImage* 54 (4), 2659–2671.
- Libby, P., Ridker, P.M., Maseri, A., 2002. Inflammation and atherosclerosis. *Circulation* 105 (9), 1135–1143.
- Lind, L., 2008. Endothelium-dependent vasodilation, insulin resistance and the metabolic syndrome in an elderly cohort: the Prospective Investigation of the Vasculature in Uppsala Seniors (PIVUS) study. *Atherosclerosis* 196 (2), 795–802.
- Maruyama, K., Uchiyama, S., Iwata, M., 2009. Metabolic syndrome and its components as risk factors for first-ever acute ischemic noncardioembolic stroke. *J. Stroke Cerebrovasc. Dis.* 18 (3), 173–177.
- McIntosh, A.R., Lobaugh, N.J., 2004. Partial least squares analysis of neuroimaging data: applications and advances. *NeuroImage* 23, S250–S263.
- McIntosh, E.C., Jacobson, A., Kemmotsu, N., Pongpipat, E., Green, E., Haase, L., Murphy, C., 2017. Does medial temporal lobe thickness mediate the association between risk factor burden and memory performance in middle-aged or older adults with metabolic syndrome? *Neurosci. Lett.* 636, 225–232.
- Meigs, J.B., 2000. Invited commentary: insulin resistance syndrome? Syndrome X? Multiple metabolic syndrome? A syndrome at all? Factor analysis reveals patterns in the fabric of correlated metabolic risk factors. *Am. J. Epidemiol.* 152 (10), 908–911.
- Meigs, J.B., D'Agostino, R.B., Wilson, P.W., Cupples, L.A., Nathan, D.M., Singer, D.E., 1997. Risk variable clustering in the insulin resistance syndrome: the Framingham Offspring Study. *Diabetes* 46 (10), 1594–1600.
- Palombo, D., Hayes, S., Peterson, K., Keane, M., Verfaellie, M., 2016. Medial temporal lobe contributions to episodic future thinking: scene construction or future projection? *Cereb. Cortex*.
- Park, J.-H., Kwon, H.-M., 2008. Association between metabolic syndrome and previous ischemic lesions in patients with intracranial atherosclerotic stroke. *Clin. Neurol. Neurosurg.* 110 (3), 215–221.
- Preul, C., Lohmann, G., Hund-Georgiadis, M., Guthke, T., von Cramon, D.Y., 2005. Morphometry demonstrates loss of cortical thickness in cerebral microangiopathy. *J. Neurol.* 252 (4), 441–447.
- Raffaitin, C., Gin, H., Empaña, J.-P., Helmer, C., Berr, C., Tzourio, C., ... Barberger-Gateau, P., 2009. Metabolic syndrome and risk for incident Alzheimer's disease or vascular dementia the Three-City Study. *Diabetes Care* 32 (1), 169–174.
- Reid, A.T., van Norden, A.G., de Laat, K.F., van Oudheusden, L.J., Zwiers, M.P., Evans, A.C., ... Kötter, R., 2010. Patterns of cortical degeneration in an elderly cohort with cerebral small vessel disease. *Hum. Brain Mapp.* 31 (12), 1983–1992.
- Rosas, H., Liu, A., Hersch, S., Glessner, M., Ferrante, R., Salat, D., ... Fischl, B., 2002. Regional and progressive thinning of the cortical ribbon in Huntington's disease. *Neurology* 58 (5), 695–701.
- Sakkinen, P.A., Wahl, P., Cushman, M., Lewis, M.R., Tracy, R.P., 2000. Clustering of procoagulation, inflammation, and fibrinolysis variables with metabolic factors in insulin resistance syndrome. *Am. J. Epidemiol.* 152 (10), 897–907.
- Salat, D.H., Buckner, R.L., Snyder, A.Z., Greve, D.N., Desikan, R.S., Busa, E., ... Fischl, B., 2004. Thinning of the cerebral cortex in aging. *Cereb. Cortex* 14 (7), 721–730.
- Salat, D.H., Williams, V.J., Leritz, E.C., Schnyer, D.M., Rudolph, J.L., Lipsitz, L.A., ... Milberg, W.P., 2012. Inter-individual variation in blood pressure is associated with regional white matter integrity in generally healthy older adults. *NeuroImage* 59 (1), 181–192.
- Saute, R., Soder, R., Alves Filho, J., Baldissotto, M., Franco, A., 2016. Increased Brain Cortical Thickness Associated With Visceral Fat in Adolescents. *Pediatric Obesity*.
- Ségonne, F., Dale, A., Busa, E., Glessner, M., Salat, D., Hahn, H., Fischl, B., 2004. A hybrid approach to the skull stripping problem in MRI. *NeuroImage* 22 (3), 1060–1075.
- Ségonne, F., Pacheco, J., Fischl, B., 2007. Geometrically accurate topology-correction of cortical surfaces using nonseparating loops. *IEEE Trans. Med. Imaging* 26 (4), 518–529.
- Seo, S.W., Lee, J.-M., Im, K., Park, J.-S., Kim, S.-H., Kim, S.T., ... Kim, J.H., 2012. Cardiovascular risk factors cause cortical thinning in cognitively impaired patients: relationships among cardiovascular risk factors, white matter hyperintensities, and cortical atrophy. *Alzheimer Dis. Assoc. Disord.* 26 (2), 106–112.
- Shen, B.-J., Todaro, J.F., Niaura, R., McCaffery, J.M., Zhang, J., Spiro III, A., Ward, K.D., 2003. Are metabolic risk factors one unified syndrome? Modeling the structure of the metabolic syndrome X. *Am. J. Epidemiol.* 157 (8), 701–711.
- Sled, J.G., Zijdenbos, A.P., Evans, A.C., 1998. A nonparametric method for automatic correction of intensity nonuniformity in MRI data. *IEEE Trans. Med. Imaging* 17 (1), 87–97.
- Song, S.-W., Chung, J.-H., Rho, J.S., Lee, Y.-A., Lim, H.-K., Kang, S.-G., ... Kim, S.-H., 2015. Regional cortical thickness and subcortical volume changes in patients with metabolic syndrome. *Brain Imaging Behav.* 9 (3), 588–596.
- Tchistiakova, E., Anderson, N.D., Greenwood, C.E., MacIntosh, B.J., 2014. Combined effects of type 2 diabetes and hypertension associated with cortical thinning and impaired cerebrovascular reactivity relative to hypertension alone in older adults. *NeuroImage Clin.* 5, 36–41.
- Tchistiakova, E., MacIntosh, B.J., Initiative, A.S.D.N., 2016. Summative effects of vascular risk factors on cortical thickness in mild cognitive impairment. *Neurobiol. Aging* 45, 98–106.

- Team, R. C., 2015. R: A Language and Environment for Statistical Computing. 2012 R Foundation for Statistical Computing, Vienna URL: <http://www.R-project.org>.
- Tesaro, M., Cardillo, C., 2011. Obesity, blood vessels and metabolic syndrome. *Acta Physiol.* 203 (1), 279–286.
- van Velsen, E.F., Vernooij, M.W., Vrooman, H.A., van der Lugt, A., Breteler, M.M., Hofman, A., ... Ikram, M.A., 2013. Brain cortical thickness in the general elderly population: the Rotterdam Scan Study. *Neurosci. Lett.* 550, 189–194.
- Veit, R., Kullmann, S., Heni, M., Machann, J., Häring, H.-U., Fritsche, A., Preissl, H., 2014. Reduced cortical thickness associated with visceral fat and BMI. *NeuroImage Clin.* 6, 307–311.
- Verstynen, T.D., Weinstein, A., Erickson, K.I., Sheu, L.K., Marsland, A.L., Gianaros, P.J., 2013. Competing physiological pathways link individual differences in weight and abdominal adiposity to white matter microstructure. *NeuroImage* 79, 129–137.
- Vuorinen, M., Kåreholt, L., Julkunen, V., Spulber, G., Niskanen, E., Paajanen, T., ... Solomon, A., 2013. Changes in vascular factors 28 years from midlife and late-life cortical thickness. *Neurobiol. Aging* 34 (1), 100–109.
- Waldstein, S.R., Lefkowitz, D.M., Siegel, E.L., Rosenberger, W.F., Spencer, R.J., Tankard, C.F., ... Katzel, L.I., 2010. Reduced Cerebral Blood Flow in Older Men with Higher Levels of Blood Pressure. *J. Hypertens.* 28 (5), 993–998.
- Wild, S.H., Byrne, C.D., Tzoulaki, I., Lee, A.J., Rumley, A., Lowe, G.D., Fowkes, F.G.R., 2009. Metabolic syndrome, haemostatic and inflammatory markers, cerebrovascular and peripheral arterial disease: The Edinburgh Artery Study. *Atherosclerosis* 203 (2), 604–609.
- Williams, V.J., Leritz, E.C., Shepel, J., McGlinchey, R.E., Milberg, W.P., Rudolph, J.L., ... Salat, D.H., 2013. Interindividual variation in serum cholesterol is associated with regional white matter tissue integrity in older adults. *Hum. Brain Mapp.* 34 (8), 1826–1841.
- Wolf, E.J., Sadeh, N., Leritz, E.C., Logue, M.W., Stoop, T.B., McGlinchey, R., ... Miller, M.W., 2016. Posttraumatic stress disorder as a catalyst for the association between metabolic syndrome and reduced cortical thickness. *Biol. Psychiatry* 80 (5), 363–371.
- Wonderlick, J., Ziegler, D.A., Hosseini-Varnamkhasti, P., Locascio, J., Bakkour, A., Van Der Kouwe, A., ... Dickerson, B.C., 2009. Reliability of MRI-derived cortical and subcortical morphometric measures: effects of pulse sequence, voxel geometry, and parallel imaging. *NeuroImage* 44 (4), 1324–1333.
- Yaffe, K., 2007. Metabolic syndrome and cognitive disorders: is the sum greater than its parts? *Alzheimer Dis. Assoc. Disord.* 21 (2), 167–171.
- Yaffe, K., Kanaya, A., Lindquist, K., Simonsick, E.M., Harris, T., Shorr, R.I., ... Newman, A.B., 2004. The metabolic syndrome, inflammation, and risk of cognitive decline. *JAMA* 292 (18), 2237–2242.
- Yates, K.F., Sweat, V., Yau, P.L., Turchiano, M.M., Convit, A., 2012. Impact of metabolic syndrome on cognition and brain: a selected review of the literature. *Arterioscler. Thromb. Vasc. Biol.* 32 (9), 2060–2067.